



New Paleocene–Eocene paleomagnetic results from the foreland of the Southern Alps confirm decoupling of stable Adria from the African plate

Emő Márton ^{a,*}, Dario Zampieri ^b, Miklós Kázmér ^c, István Dunkl ^d, Wolfgang Frisch ^e

^a Eötvös Loránd Geophysical Institute of Hungary, Paleomagnetic Laboratory, Columbus 17-23, H-1145 Budapest, Hungary

^b Department of Geosciences, University of Padova, Via Gradenigo 6, 35131 Padova, Italy

^c Department of Palaeontology, Eötvös University, Pázmány Péter sétány 1/c, H-1117 Budapest, Hungary

^d Sedimentology & Environmental Geology, Geoscience Center, University of Göttingen, Goldschmidtstraße 3, D-37077 Göttingen, Germany

^e Institut für Geologie und Paläontologie, University of Tübingen, Sigwartstraße 10, D-72076 Tübingen, Germany

ARTICLE INFO

Article history:

Received 5 November 2010

Received in revised form 25 February 2011

Accepted 3 March 2011

Available online 11 March 2011

Keywords:

Adria

Paleocene

Eocene

Paleomagnetism

CCW rotation

ABSTRACT

From the “undeformed” foreland of the Southern Alps Paleocene through Early Miocene rocks, mostly biostratigraphically well-dated sediments with sub-horizontal bed attitude were collected for a paleomagnetic study from 23 geographically distributed localities. The samples were subjected to standard paleomagnetic measurements and evaluation. While the Miocene samples are unstable, most of the older localities yielded statistically well-defined paleomagnetic directions. These are interpreted as primary for the compact marls, supported by positive between-locality tilt and reversal tests. This large group of localities is characterized by CCW rotated declinations with respect to the present north. Combined with paleomagnetic directions of corresponding age from stable Istria, these allow definition of the APW for stable Adria for the 61.6–33.9 Ma interval, which is significantly displaced from the coeval segment of the African APW due to the decoupling of the former to the latter by a moderate CCW rotation. This post-Eocene final separation (exact age is not constrained directly, but estimated as end-of-Miocene) was preceded by a small CW rotation of Adria with respect to Africa, suggested by unchanged orientation of the former across the Cretaceous–Paleocene boundary, while the latter continued its CCW rotation.

© 2011 Elsevier B.V. All rights reserved.

1. Introduction

In recent years a systematic paleomagnetic study was carried out on geographically distributed Late Jurassic–Late Cretaceous localities from the foreland of the Southern Alps (Adige embayment), which belongs to stable Adria. The results were combined with coeval paleomagnetic results from another exposed area of stable Adria, which is in the Istria peninsula (Márton et al., 2008, 2010). The apparent polar wander (APW) path thus defined was displaced in a counter-clockwise (CCW) sense with respect to the African APW (Besse and Courtillot, 2002) by about 10°. This was interpreted as the resultant of a Latest Cretaceous CW and a post-Eocene CCW rotation, since the CCW rotation exhibited by Eocene rocks from stable Istria (Márton et al., 2003) was larger than the CCW rotation measured on the Late Cretaceous rocks from the same region.

In a pioneer work, Soffel (1972) investigated igneous rocks from the Euganei Hills, representing the foreland of the Southern Alps. This was followed by a number of papers dealing also with the

paleomagnetism of the volcanites from other parts of the same foreland, the Berici and Lessini Mts (Soffel, 1974, 1975a, 1975b, 1975c). From the highly scattered paleomagnetic directions (the scatter was attributed to the secular variation of the Earth's magnetic field) he concluded that the area rotated in the CCW sense with respect to stable Europe during the Eocene–Oligocene volcanic activity. His data were re-interpreted by Channell et al. (1978), who, in the light of new K/Ar ages, argued that such rotation did not exist. At the same time Soffel (1978) pointed out that the “clearly” Oligocene and “clearly” Eocene overall mean paleomagnetic directions, which are based on well-grouped site mean directions (both accompanied by more scattered “satellite” directions) are statistically different and imply at least 20–30° CCW rotation between the Eocene and the Early to middle Oligocene.

The obvious purpose of the paleomagnetic investigations in such situation would have been to study the Paleogene sediments from the foreland of the Southern Alps, which did not happen till the present time. In this paper we are presenting new paleomagnetic results from the post-Cretaceous sediments of the Euganei Hills and also from the two other uplifted parts of the Adige embayment, the Lessini and Berici Mts. In addition, new results will be presented for some igneous rocks, outcropping close to studied sediments, basically to document that the sediments were not re-magnetized during the igneous activity.

* Corresponding author. Fax: +36 1 2480378.

E-mail addresses: paleo@elgi.hu (E. Márton), dario.zampieri@unipd.it (D. Zampieri), mkazmer@gmail.com (M. Kázmér), istvan.dunkl@geo.uni-goettingen.de (I. Dunkl), frisch@uni-tuebingen.de (W. Frisch).

2. Geological setting

The Alpine belt originated from the Late Cretaceous to Present convergence between the Adriatic upper plate and the subducting European lower plate (e.g., Dal Piaz et al., 2003; Dewey et al., 1989; Kurz et al., 1998). It is composed of a Europe-vergent collisional wedge (Alpine domain s.s.) and a south-propagating fold-and-thrust belt (South Alpine domain) separated by a major fault system, the Periadriatic Lineament (Fig. 1).

During the first stages of the Alpine orogeny (Late Cretaceous–Early Paleocene), the central and western Southern Alps constituted the slightly deformed hinterland of the Europe-vergent Austroalpine–Penninic collisional wedge. From the Miocene onward (Nealpine phase), the Southern Alps were shortened as a south-vergent fold-and-thrust belt, which developed as a retro-wedge (Castellarin et al., 2006; Doglioni and Bosellini, 1987).

The Southern Alps are subdivided into two main sectors (Lombardian and Venetian) by the NNE–SSW-trending Giudicarie belt (Fig. 1). In between the two sectors, the triangular swell of the Adige embayment comprising the Lessini and Berici Mountains and the Euganei Hills represents the “undeformed” foreland of the Southern Alps (Bigi et al., 1990; Castellarin et al., 2006; Fantoni and Franciosi, 2009) and thus the autochthonous core of the Adriatic plate.

Despite the Alpine shortening, the Southern Alps preserved the different paleogeographic units of the Mesozoic Adriatic passive margin. From east to west they are the Julian Basin, the Friuli Platform (part of the Adriatic Carbonate Platform, see Cati et al., 1989), the Belluno Basin, the Trento Platform and the Lombardian basin (e.g., Bertotti et al., 1993). The Trento Platform was drowned during the Middle Jurassic and became a seamount (Trento Plateau).

During the complex collision between Europe and Adria, the inherited structural setting of the margins has controlled the final tectonic pattern along with the distribution of the sedimentary facies. The former Trento Plateau (to which the Lessini and Berici Mts and the Euganei Hills belong) reacted rigidly during the collision and was

affected by block-faulting, which progressively reduced its extension. The uplifted blocks acted as centers of shallow-water carbonate sedimentation, which prograded and coalesced giving rise to the “Lessini shelf”, a resurrected platform with scattered reefs, lagoons, islands and volcanoes (Bosellini, 1989), corresponding to the present-day Lessini and Berici Mts. The volcanic activity in the Lessini shelf is connected to Paleogene extension (De Vecchi et al., 1976). The main extensional structure is the NNW-trending Alpone–Agno graben located in the eastern Lessini Mountains and bounded to the west by the Castelvero normal fault (Fig. 2). The extensional deformation produced a widespread network of normal faults, either planar (domino style) or listric with low to moderate tilting of blocks (Zampieri, 1995). In the eastern Lessini Mts mafic and ultramafic rocks erupted during the Late Paleocene–Late Eocene, mainly in submarine environments. During the Late Eocene on the flanks of emerged volcanic ridges marine transgressive sediments were deposited (“Marne di Priabona”). The volcanic activity continued in the Early Oligocene east of Schio, in the Berici Mountains and in the Euganei Hills (De Vecchi et al., 1976).

After the Eocene the tectonic control on the accommodation space along with eustatic sea-level fluctuations produced strong variations of sediment facies and thickness, even on short distances. In the eastern Lessini and Berici Mountains the Lower Oligocene “Calcareni di Castelgomberto” Formation (platform carbonates ca. 200 m thick) deposited on the Marne di Priabona or directly on the volcanics, where the Priabonian marls are missing. At the beginning of the Late Oligocene the Calcareni di Castelgomberto carbonate platform became emergent and submitted to deep paleokarst development, testified in the eastern Lessini by cavities and dolines infilled by quartz sandstones (Frost, 1981). The unconformity is overlain by coralline algal rudstones (“Arenarie e Calcarei di S. Urbano”) of Late Oligocene age (Bassi et al., 2007). These are in turn overlain by marly and shaly sediments (“Marne argillose del M. Costi”) of Early Miocene age (Bassi et al., 2008), which were also deposited in shallow-water environment, yet documenting the cessation of carbonate platform

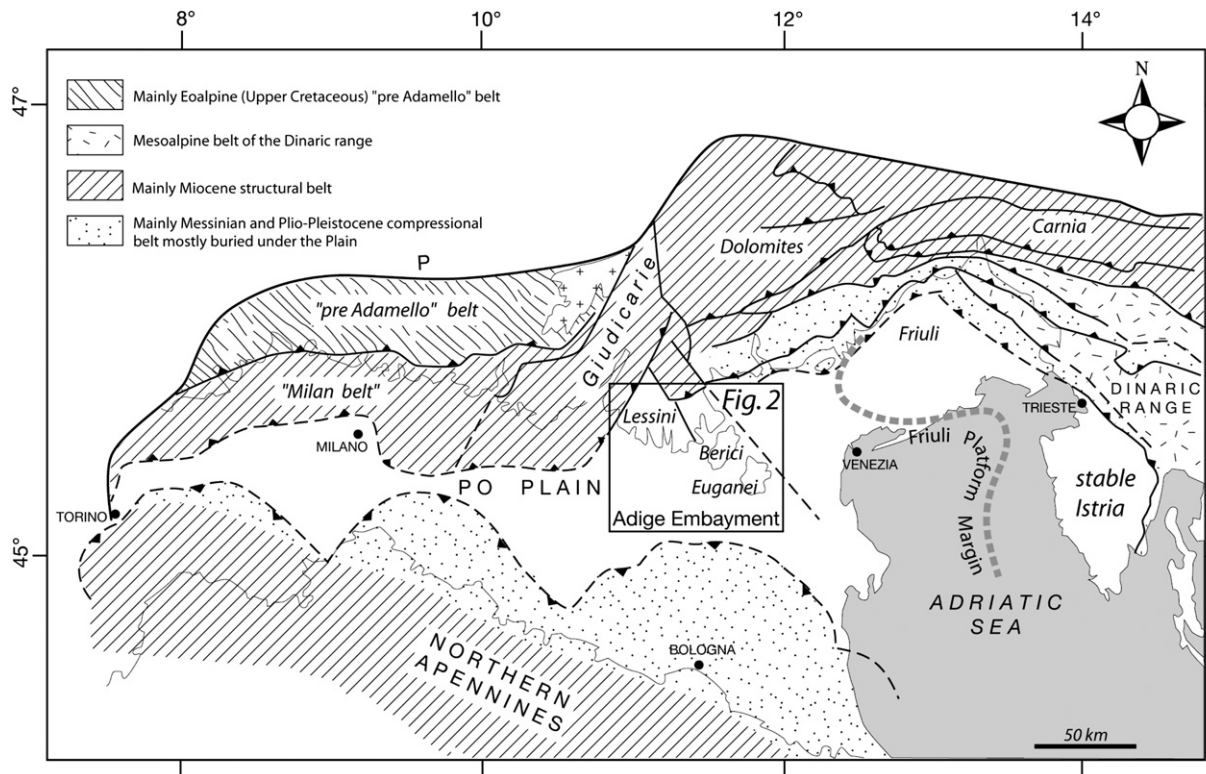


Fig. 1. Structural sketch of the Southern Alps, Northern Apennines and Northern Dinaric range with their partly common foreland areas (after Castellarin et al., 2006). The central inset shows the study area of Fig. 2, i.e. the Adige embayment.

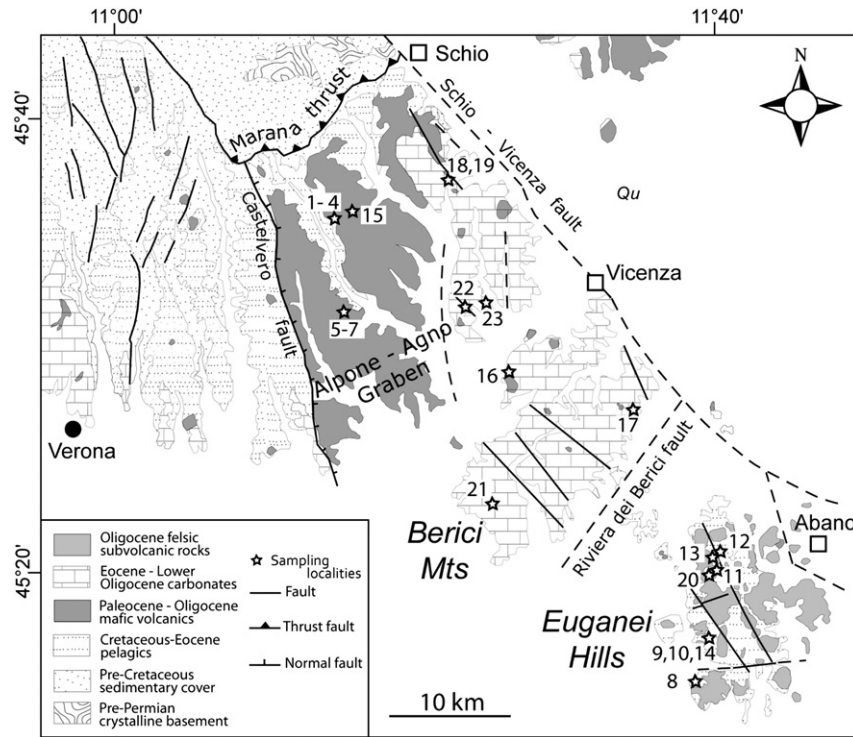


Fig. 2. Simplified geological map of the study area with the paleomagnetic sampling localities, according to Table 1. Legend: Ages are 1–4: Paleocene, 5–10: Ypresian, 11–14: Lutetian, 15–19: Priabonian, 20 and 21: Oligocene, and 22 and 23: Aquitanian. The numbers are used throughout the paper.

sedimentation, probably controlled by a climatic lowering of sea-water temperature (Bassi et al., 2007; Bosellini, 1989).

Southeast of the Riviera dei Berici fault (Fig. 2), in the area of Euganei Hills, Lower Eocene to Lower Oligocene “Marne Euganee” (marls with nummulitic limestone intercalations) were deposited in basinal conditions (Massari et al., 1977). In the area they represent the youngest sedimentary deposits cropping out from the Quaternary alluvial plain.

3. Stratigraphic position of the sampling localities

The oldest rocks sampled for the present study are from the Paleocene S. Daniele section (Lessini Mts, localities 1–4) lying within the Alpone-Agno graben (Fig. 2), which was studied in the late seventies by biostratigraphic analysis (Zampieri, 1979). The section starts with a well-developed Maastrichtian hardground, at the top of



Fig. 3. West facing wall of the Lovara quarry, located on the west slope of the Chiampo valley (Vicenza). Legend: The quarry exploited the “nummulitic limestones” commercially known as “Chiampo marble”, of which some blocks are seen in the foreground. The sampled layer (locality 5) is indicated by white arrows. The drilling was made just to the left (north) of the left margin of the photo, in the same layer which in the central part of the photo is suturing a scour structure incised in the limestone. The top of the layer shows intense bioturbation and hardground development. The sediment infilling the scour is firstly a cross-bedded grainstone (central part of the photo), then a red shale (right side) with planktonic foraminifera of Ypresian age.

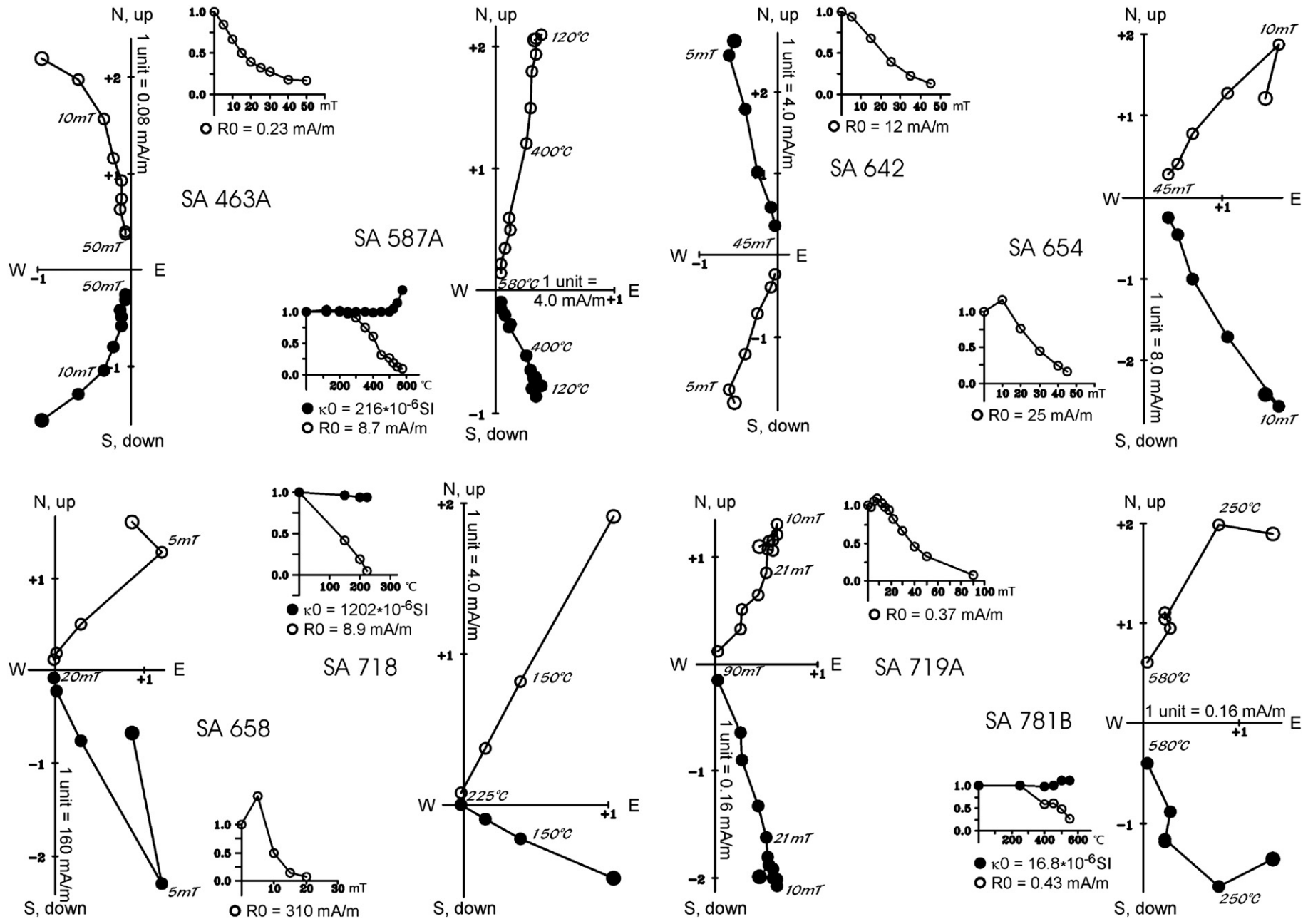


Fig. 4. Typical demagnetization curves from the study area. Legend: examples are from localities 1 (SA 642), 2 (SA654), 3 (SA 658), 5 (SA 781B), 6 (SA719A), 11 (SA 587A), 15 (SA 718) and 18 (SA 463A). Zijderveld diagrams are in the geographic system: full dots: projection of the NRM vector onto the horizontal, circles: into the vertical. Zijderveld diagrams are accompanied by intensity (circles) versus demagnetizing field diagrams, when the method of demagnetization is AF, and by NRM intensity (circles)/susceptibility (dots) versus temperature diagrams, when the method of demagnetization is thermal.

the Scaglia Rossa hemipelagic unit. It is followed by a 1.5 m thick chaotic bed with Scaglia rossa clasts inside a clay matrix indicating tectonic activity and the formation of fault scarps, corresponding to the first phase of development of the graben. The section continues with 2 m of fine-grained volcanoclastics (locality 1) of Middle Paleocene age (according to the planktonic foraminiferal content) and an olistolite of Scaglia Rossa cut by two basaltic dikes (localities 3 and 4) injected along normal faults. Some meters of coarse-grained volcanoclastics are followed by dm-thick beds of violet limestones intercalated within red calcareous marls (locality 2) with the same Middle Paleocene age (also constrained by planktonic foraminifera).

From the Alpone-Agno graben a younger section was sampled in the inactive Lovara quarry, west of Chiampo (Fig. 2, localities 5–7). The quarrying exploited the “nummulitic limestone”, which represents the deposit of channelized bioclastic sands produced on the ramp margin of a carbonate platform but deposited in a basin. A detailed biostratigraphic analysis of the nummulitic limestone in the Lovara quarry (Beccaro et al., 2001) yielded Ypresian age. From this quarry the following rocks were sampled: a gray packstone–grainstone of biostratigraphically controlled Ypresian age (locality 6), a purple fine-grained clayey limestone (locality 5) below it, which is capping a scour filled by cross-bedded grainstone (Fig. 3), and is underlain by Eocene volcanoclastics (not visible in the quarry) and the basalt tuff above the gray limestone (locality 7).

From the Alpone-Agno graben, a dark gray clay (without fossils) derived from early weathering of Eocene mafic volcanics was also sampled (locality 15). The age of this clay is estimated as Priabonian, since the parent rock is probably of Middle Eocene age (the underlying volcanics contain intercalated Ypresian nummulitic limestone).

In the easternmost Lessini Mts, in Priabona village, Priabonian sediments were drilled below the church (locality 18) and in the inactive quarry (Priabonian type locality) northwest of the village (locality 19). Both outcrops lie below the base of the Lower Oligocene carbonate platform, which is also the stratigraphic position of the Altavilla Vicentina (locality 16) and Lumignano marls (locality 17) in the Berici Hills. In the same hills, inside a karst paleovalley (Pozzolo valley) incised on the Lower Oligocene carbonate platform, fluvial

sediments of Late Oligocene age were sampled in an inactive quarry (locality 21). Marly limestones of Aquitanian age (Marne di M. Costi) were drilled in the southeastern Lessini Mts close to S. Urbano (locality 22) and on the ridge north of Sovizzo (locality 23).

The sediments sampled in the Euganei Hills are the Lower Eocene p.p. to Lower Oligocene “Marne Euganee”. This unit was sampled at several localities (Fig. 2): Piomba quarry, close to Este (locality 8), road cut southwest of Teolo (locality 11), creek east of Teolo (locality 12), school yard, south of Teolo (locality 13), and Cocuzzola quarry (close to Fontanafredda), where marls (locality 9) and dark gray clay (locality 14) were drilled. Marls were also collected at Santa Lucia, in a new building site (locality 10). We also sampled a trachytic intrusion of Oligocene age (locality 20) near locality 11.

4. Paleomagnetic sampling, laboratory processing and results

As the previous section documents, the sampling localities are geographically distributed in the foreland of the Southern Alps. Although they mostly represent the Paleocene–Eocene time interval, there are some localities, which are of Oligocene or of Miocene age. The total number of the sampled localities is 23, and the number of independently oriented (mostly with the magnetic method) drill cores is 240.

The drill cores were cut into standard-size specimens in the laboratory. The natural remanent magnetization (NRM) of each specimen was measured using JR-4 and JR-5A magnetometers. Sisters of pilot specimens from each group were demagnetized in increments, one with thermal, the other with alternating field (AF) method. The rest of the samples from the respective localities were also stepwise demagnetized with the method which yielded the better defined demagnetization curves. The curves were analyzed for linear segments (Kirschvink, 1980) and the components were subjected to statistical analysis. In most of the studied samples the NRM was a single component (Fig. 4, all examples, except SA463A). When the stable or high blocking component was overprinted (e.g., Fig. 4, SA463A), the characteristic remanence was identified as the practically linear component decaying toward the origin.

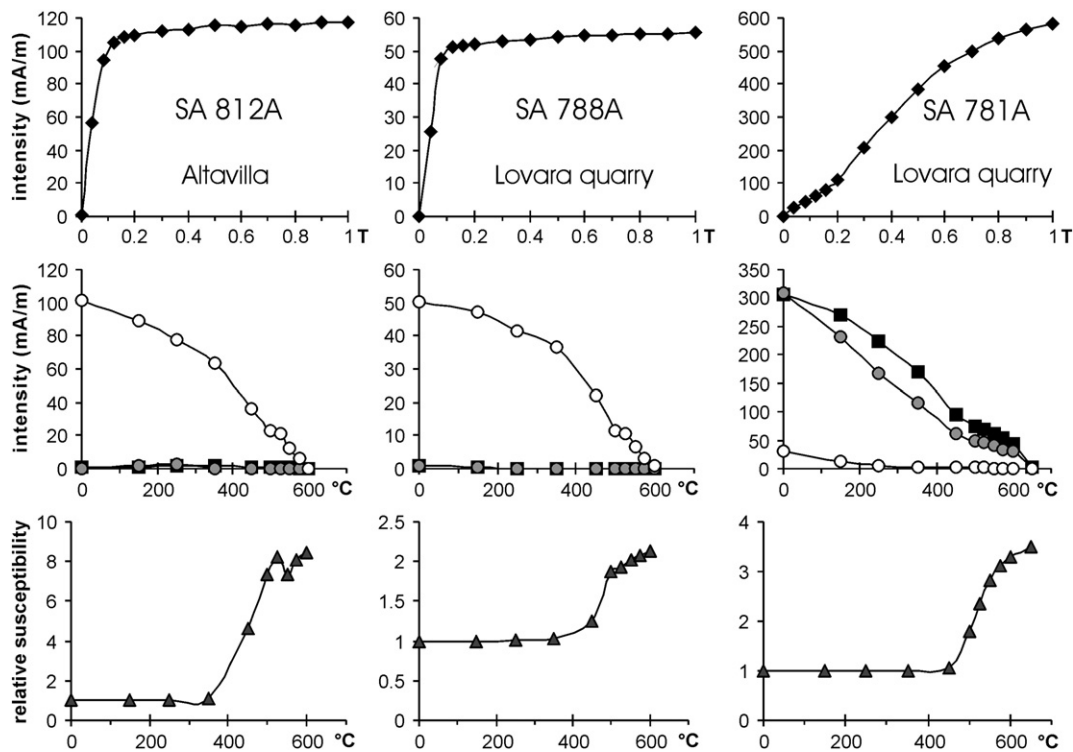


Fig. 5. Examples of IRM acquisition, the behaviour of the three component IRM (Lowrie, 1990) on stepwise thermal demagnetization and the susceptibility monitored during heating. Legend: components of the IRM were acquired in fields of 1 T (squares), 0.36 T (dots) and 0.12 T (circles), respectively.

The magnetic mineralogy experiments included the stepwise magnetization of the specimens up to 1.0 T field (IRM) and the stepwise thermal demagnetization of the 3-component IRM (Lowrie, 1990) accompanied by monitoring the susceptibility change on heating (Fig. 5). In addition, some information about the actual carrier of the NRM was obtained from the behaviour of the NRM and the susceptibility on thermal demagnetization. These experiments show that the most common magnetic mineral in the sediments as well as in the igneous rocks is magnetite, which is also the carrier of the NRM. The notable exceptions are locality 15, where the NRM

resides in a magnetic iron sulphide (Fig. 3 SA718), and locality 5 (Fig. 5, SA781A), where the hard/medium hard components are dominant in the IRM and they decay only at the Curie-point of the hematite.

Concerning the paleomagnetic results, there are a few localities which failed to yield positive results, either because of extremely weak signal (locality 17), or for instability of the NRM on demagnetization (localities 4, 13, 14, 21, 22, and 23). The remaining localities are characterized by mean paleomagnetic directions with good or excellent statistical parameters. For localities 7 and 16 two directions are tabulated (Table 1). In the first case, the magnetically

Table 1
Summary of locality mean paleomagnetic directions for the Foreland of the Southern Alps (Adige embayment) based on the results of principal component analysis (Kirschvink, 1980). Localities are numbered according to Fig. 2.

Locality	Lat. N, Lon. E	n/no	D°	I°	k	α_{95} °	D _c °	I _c °	k	α_{95} °	Dip		
<i>Paleocene</i>													
1	S. Daniele, dark gray-greenish tuff, SA 642–647	45° 34' 40" 11° 16' 27"	5/6	350	+40	126	7	353	+42	126	7	110/4	
2	S. Daniele, red marl SA 648–654	45° 34' 40" 11° 16' 26"	7/7	165	–35	77	7	167	–37	77	7	110/4	
3	S. Daniele, basalt dike ** SA 658–663	45° 34' 39" 11° 16' 25"	5/6	164	–24	92	8	165	–26	92	8	110/4?	
4	S. Daniele, basalt dike ** SA 664–673	45° 34' 40" 11° 16' 25"	0/10	Large scatter, unstable									110/4?
<i>Ypresian</i>													
5	Lovara quarry, purple limestone, SA 779–786	45° 32' 13" 11° 15' 59"	5/8	154	–49	38	12	149	–43	38	12	295/8	
6	Lovara quarry, gray SA 719–722, 787–792	45° 32' 12" 11° 15' 55"	10/10	152	–30	34	8	157	–38	36	8	113/11	
5+6	Lovara quarry, combined		15/18	153	–36	25	8	154	–40	35	6		
7	Lovara quarry, basalt tuff, SA 723–731	45° 32' 12" 11° 15' 55"	a 5/9 b 7/9	340 180	+57 –52	52 120	11 6	340 180	+57 –52	52 120	11 6	Horizontal	
8	Este, Cava Piomba SA 439–447	45° 15' 36" 11° 39' 08"	5/9	329	+40	51	11	325	+39	51	11	250/5	
9	Cocuzzola, marl SA 674–683	45° 17' 05" 11° 39' 47"	7/10	148	–31	53	8	157	–50	53	8	124/21	
10	Sta. Lucia, V. Chiesa, marl SA 622–641	45° 16' 53" 11° 39' 46"	10/20	313	+52	19	11	310	+45	19	11	290/7	
<i>Lutetian, Marne Euganee</i>													
11	Teolo, road cut, marl SA 587–594	45° 20' 28" 11° 40' 01"	8/8	152	–65	245	4	159	–61	245	4	20/5	
12	Teolo, creek, marl SA 692–699	45° 20' 50" 11° 40' 42"	7/8	156	–43	101	6	153	–43	101	6	238/3	
13	Teolo, school, marl SA 700–713	45° 20' 28" 11° 40' 39"	0/14	Large scatter									Horizontal
14	Cocuzzola, dark gray clay SA 684–691	45° 17' 05" 11° 39' 47"	0/8	Large scatter									
<i>Priabonian</i>													
15	Monte Croce di Popi, dark gray clay, SA 714–718	*45° 36' 21" *11° 16' 52"	5/5	148	–65	44	12	148	–65	44	12	Horizontal	
16	Altavilla Vicentina, silty marl, SA 811–824	*45° 29' 53" *11° 27' 34"	a 8/14 b10/14	322 183	+50 –48	29 45	10 7	313 192	+64 –61	29 45	10 7	160/15	
17	Lumignano, marl SA 767–770	*45° 27' 28" *11° 34' 43"	0/4	Extremely weak									Horizontal
18	Priabona 1, below church SA 458–467, silty marl	*45° 38' 05" *11° 22' 22"	9/10	184	–61	146	4	198	–64	146	4	125/8	
19	Priabona 2, quarry, marl SA 612–621	*45° 38' 20" *11° 22' 00"	9/10	214	–55	43	9	225	–61	43	9	175/9	
<i>Oligocene</i>													
20	Teolo, road cut, trachyte intrusion SA 595–597	45° 20' 23" 11° 39' 57"	3/3	322	61	144	10	322	61	144	10		
21	Pozzolo, fluvial sediment SA 793–810	*45° 24' 20" *11° 29' 36"	0/18	Unstable, large scatter									206/10
<i>Aquitanian</i>													
22	S. Urbano, marne M. Costi SA 937–942	*45° 32' 41" *11° 24' 01"	0/6	Large scatter									50/10
23	Sovizzo, marne M. Costi SA 948–955	*45° 33' 06" *11° 26' 06"	0/8	Large scatter									79/11

Key: Lat. N, Lon. E: Geographic coordinates (WGS84) measured by GPS except for those marked with *, which were calculated by using Google Earth, n/no: number of used/collected samples (the samples are independently oriented cores); D, I (D_c, I_c): declination, inclination before (after) tilt correction; k and α_{95} : statistical parameters (Fisher, 1953), ** age may be younger than Paleocene: could be Eocene or even Early Oligocene.

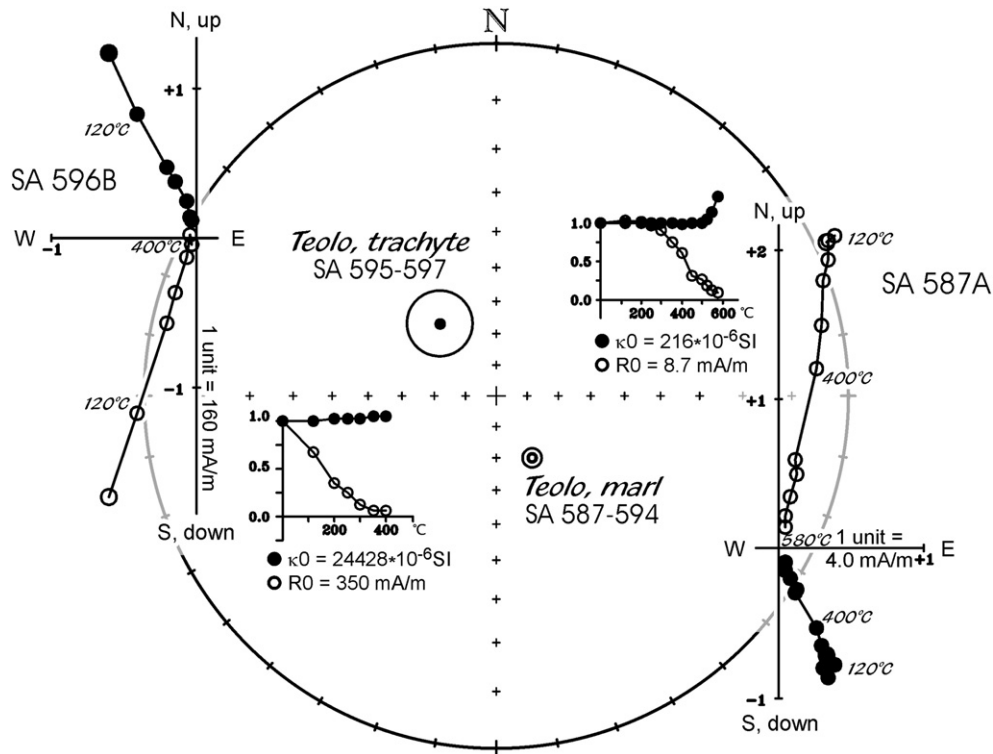


Fig. 6. Mean paleomagnetic directions of Teolo localities with α_{95} on a stereographic projection for a Lutetian marl beds and a nearby trachyte intrusion, respectively. Legend: On either side of the stereonet, typical demagnetization curves are shown for the two lithologies. Key for the demagnetization diagrams as for Fig. 4.

softer normal polarity component (7a) seems to be older than the magnetically harder, reversed polarity component (7b). For locality 16, the component analysis provides a normal polarity component (16a, which is interpreted as older), while the reversed polarity direction (16b), calculated from the end points of the demagnetization curves should be younger. Finally, it has to be mentioned that the direction for locality 19 is not calculated from components, but from the end points of the demagnetization curves, since coherent directions could not be defined from linear segments.

5. Discussion and conclusions

The Middle Paleocene S. Daniele section is represented by localities 1 and 2, which are lithologically different, but have the same sub-horizontal bedding attitude. The locality mean paleomagnetic vectors for these sediments are near-parallel, but have different polarities. The dike (locality 3) which is close to locality 1 (normal polarity) and far from locality 2 (reversed polarity) has reversed polarity remanence. Thus, remagnetization of the studied sediments of the section

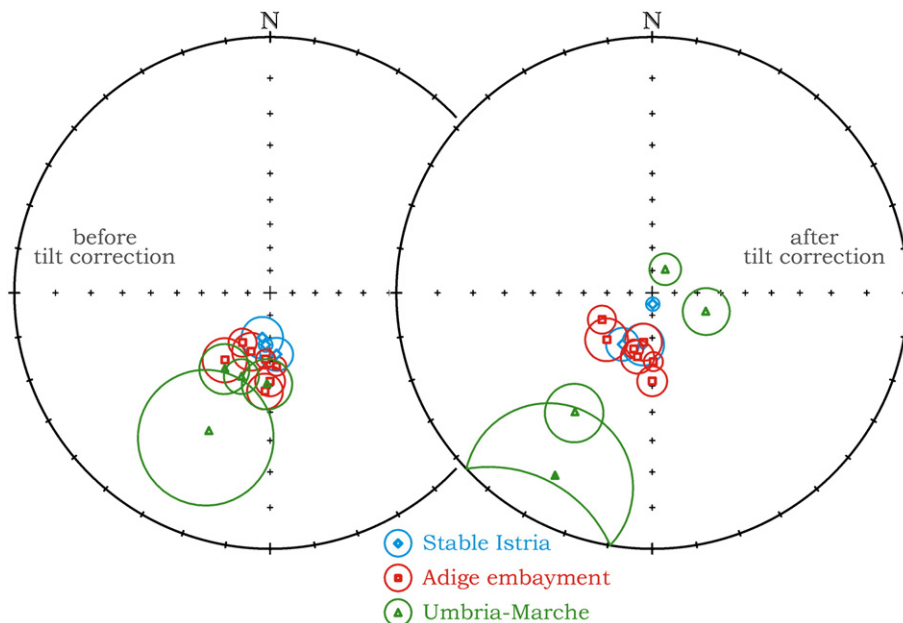


Fig. 7. Locality mean paleomagnetic directions of overprint remanences for autochthonous Istria (diamonds), for the Adige embayment (squares) and for Umbria–Marche (triangles) on stereographic net before and after tilt corrections.

Table 2
Summary of the overall mean paleomagnetic directions for the Foreland of the Southern Alps before and after tilt corrections, results of fold (McFadden, 1990) and reversal (McFadden and McElhinny, 1990) tests and paleomagnetic poles with statistical parameters.

	N	D°	I°	k	α_{95}°	D _C °	I _C °	k	α_{95}°	Parameters of McFadden fold test				Reversal test			Paleomagnetic poles				
										Is situ ξ_1	Unfolded ξ_1	Critical ξ_1 (95%)	Min ξ_1 stat.	Max k stat.	Angle between N and R	Critical angle	Class.	Lat.°	Long.°	k	α_{95}°
Paleocene–Oligocene	13	334.3	+45.9	28	8.0	335.0	+47.3	34	7.2	6.774	1.128	4.200	100%	92%	6.6	15.2	Rc	64.6	251.7	32	7.4
Paleocene–Oligocene	11	333.9	+46.4	33	8.1	334.6	+47.9	42	7.1	5.294	0.286	3.865	92%	87%	3.3	15.7	Rc	64.7	252.2	36	7.8
Paleocene–Ypresian	8	334.2	+42.2	39	8.9	334.9	44.6	48	8.1	2.483	2.028	3.298	69%	68%	6.5	17.1	Rc	62.5	246.7	37	9.3
Ypresian	6	329.3	+43.4	40	10.7	329.2	45.7	60	8.7	3.418	1.798	2.862	72%	74%	8.3	18.2	Rc	60.0	255.5	50	9.6
Ypresian–Lutetian	8	330.4	+46.1	37	9.2	330.6	47.4	57	7.4	4.710	0.710	3.298	86%	86%	7.3	15.7	Rc	62.0	256.1	50	7.9
Lutetian–Priabonian	3	332.8	+57.8	40	19.8	333.5	56.7	46	18.3	2.024	1.447	2.076	100%	100%				69.1	271.1	45	18.5
Eocene	9	330.2	+48.2	34	9.0	330.4	+49.4	49	7.4	5.030	0.358	3.497	100%	89%	7.0	16.4	Rc	63.2	259.6	44	7.9

Key as for Table 1 but N is the number of localities.

during the intrusion of the dikes can be safely excluded. The paleomagnetic declinations measured for this section suggest a moderate CCW rotation with respect to the present North.

Ypresian sediments were studied from the Lessini Mts (Lovara quarry, localities 5–7) and from the Euganei Hills (localities 8–10). The gray (locality 6) and purple (locality 5) Ypresian sediments of the Lovara quarry have opposite tilts and the tilt corrections significantly reduce the scatter of the paleomagnetic directions (Table 1, 5 + 6). The basalt tuff of high porosity (which overlies the gray limestone) exhibits two components. The magnetically softer is probably connected to the larger, primary magnetite crystals while the harder, reversed polarity component must be residing in smaller magnetite grains which are the alteration products of the mafic minerals. The paleomagnetic directions for the three different lithologies in the Lovara quarry are characterized by a moderate CCW rotation with respect to the present North and so are the paleomagnetic directions for the localities (Table 1, 8–10) of Ypresian age from the Euganei Hills.

Concerning post-Ypresian times, two localities in the Lutetian marls of the Euganei Hills yielded statistically good results. One of them (locality 11) is close to a trachyte intrusion of Oligocene age (locality 20), which could have remagnetized the sediment. However, this is not the case, since the trachyte has normal while the sediment reversed polarity remanence (Fig. 6). The Lutetian localities from the Euganei Hills are also indicative of CCW rotation, similar to a Priabonian locality (15) from the Lessini Mts.

The above discussed sediments are compact marls, mostly of basin facies. In contrast, the Priabonian localities 16–19 are near-shore silty deposits with rather high porosity, consequently more liable to remagnetization than the compact marls. Moreover, they are close to the Schio-Vicenza fault system, where fluids move. No wonder that one of the silty deposits exhibits high scatter (locality 17), another one composite NRM (locality 16), for the third components with consistent directions cannot be defined (locality 19, only the end points of the demagnetization curves yield coherent directions). Finally, it is likely that for locality 18 a secondary remanence was defined, the visible weathering was at least 20 cm in the drill cores and may have affected also the relatively fresh-looking lowermost part of the core, which was analyzed in the laboratory. In this group of localities reversed polarity magnetizations indicating small CW rotation are observed.

The localities yielding statistically well-defined paleomagnetic mean directions represent a fairly long time interval. The lower age limit of 62 Ma is well-constrained, the upper limit is estimated as 29 Ma, which is the youngest possible age for the trachyte intrusion (locality 20). The Paleocene through Lutetian part of this time interval is characterized by paleomagnetic directions which are indicative of CCW rotation, both before and after tilt corrections and so are the Priabonian locality 15 and the youngest trachyte intrusion (locality 20) of Oligocene age. We interpret, therefore, the reversed polarity components exhibited by the silty near-shore sediments and a porous basalt tuff (7b, 16b, 18 and 19) as secondary. Such interpretation is justified not only by the arguments of the previous paragraph, but also

Table 3
Summary of the overall mean paleomagnetic directions and paleomagnetic poles for stable Adria (Adige embayment + stable Istria) before and after tilt corrections calculated for each 5 Ma with a 10 Ma sliding window up to 70 Ma and for five time points with variable windows for the Tertiary segment of the APW.

Age (Ma)	N	D°	I°	k	α_{95}°	D _C °	I _C °	k	α_{95}°	Lat.°	Long.°	k	α_{95}°
37.1 ± 3.2	3	341.7	+56.5	71	14.7	337.2	+58.4	100	12.4	71.9	272.1	71	14.8
42.9 ± 5.7	5	335.6	+55.7	76	8.8	337.2	+55.4	76	8.8	71.0	263.8	65	9.6
48.1 ± 7.7	13	332.3	+50.3	42	6.5	332.9	+51.1	56	5.6	65.7	260.0	46	6.2
52.2 ± 3.8	8	330.5	+46.9	36	9.3	330.5	+48.3	54	7.6	62.4	258.3	43	8.6
55.1 ± 6.5	10	334.4	+45.2	35	8.2	334.9	+46.9	45	7.3	64.1	250.4	35	8.3
70 ± 5	5	339.2	+42.5	74	8.9	338.0	+42.0	339	4.2	62.4	239.0	550	3.3
75 ± 5	4	340.3	+44.2	78	10.5	336.9	+43.3	360	4.8	62.6	241.8	449	4.3
80 ± 5	6	336.2	+45.1	61	8.7	334.9	+45.3	198	4.8	62.7	246.9	181	5.0
85 ± 5	17	329.3	+42.8	41	5.6	334.2	+46.6	64	4.5	63.5	246.9	55	4.9
90 ± 5	24	328.4	+38.3	35	5.1	332.8	+45.0	58	3.9	61.8	251.1	50	4.2
95 ± 5	14	325.7	+35.4	34	7.0	330.2	+41.4	67	4.9	58.0	251.0	56	5.4
100 ± 5	11	328.2	+40.9	44	7.0	330.2	+41.7	105	4.5	58.1	251.9	88	4.9
105 ± 5	6	333.8	+41.1	53	9.3	329.5	+42.1	168	5.2	57.9	253.8	151	5.5

Key as for Table 1 but I_C° is corrected for compaction effect for localities younger than 94, and older than 55.1 Ma from the Adige embayment. Lat. and long. are the coordinates of the paleomagnetic pole. N is the number of localities. Note that the post-Cretaceous results are coming from sub-horizontal strata, therefore the improvement of the statistical parameters after tilt corrections is slight, compared to the Cretaceous results. In case of 42.9 Ma, none of the dip angles exceeds 5°, which explains why the statistical parameters are the same before and after tilt correction.

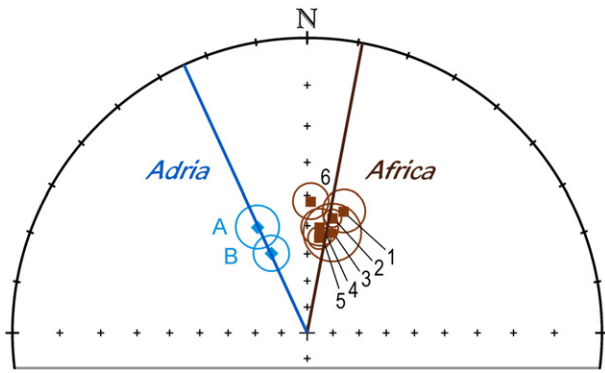


Fig. 8. Comparison between Paleocene–Early Eocene (A) and Mid–Late Eocene (B) overall-mean paleomagnetic directions based on the combination of locality mean paleomagnetic directions from autochthonous Istria and from the foreland of the Southern Alps (Adige embayment), on one hand and expected paleomagnetic directions calculated from African paleomagnetic directions of Eocene age. Legend: 1: by Lotfy (1999) (Late Eocene), 2: by Lotfy and Van der Voo (2007) (Mid–Late Eocene), 3: by Kafafy et al. (1995), 4: by Tauxe et al. (1983) (35–40 Ma), 5: by Abdeldayem (1999) (35–50 Ma) and 6: by Tauxe et al. (1983) (40–45 Ma).

by the frequent appearance of similar NRM components of Reversed polarity in the Cretaceous platform (Istria) and basin (Adige embayment) sediments (Márton et al., 2010) and in the Apennines (Satolli et al., 2007). The paleomagnetic directions 7b, 16b, 18 and 19 of the present study combined with those observed on Cretaceous rocks cluster close to $D = 192^\circ$ and $I = -57^\circ$ ($k = 40$, $\alpha_{95} = 6^\circ$) before while they become scattered after tilt corrections (Fig. 7).

The tight grouping (except one locality from Umbria–Marche) and the invariably reversed polarity suggest that they were acquired during a short interval, the direction itself that the process postdates the final CCW rotation of the Adriatic microplate. The best candidate for triggering such widespread re-magnetization may be the Messinian salinity crisis, which started at 5.96 Ma (Krijgsman et al., 1999), during a reversed polarity interval prevailing till 5.33 Ma (Ogg et al., 2008). During the crisis, there was a general sea level drop, which left exposed a broad relief (Ghielmi et al., 2009) affected by the weathering and deep karstification of the carbonate rocks (e.g., Audra et al., 2004). The Messinian unconformity is clearly seen in industrial seismic profiles of the Venetian–Friulian basin (Ghielmi et al., 2009; Mancin et al., 2007).

Having omitted the paleomagnetic directions interpreted as secondary, there are 13 localities from the foreland of the Southern Alps which can be further evaluated from the viewpoint of the age of the acquisition of the remanence. Although the tilts are mostly sub-horizontal, McFadden's (1990) fold test (for localities with shallow tilts) is positive for the 13 Paleocene–Early Oligocene localities as well as for the 11 sedimentary localities. The reversal tests (McFadden and McElhinny, 1990) are also positive (Table 2). Thus, both tests point to the primary nature of the NRMs in question.

The 11 sedimentary localities represent a fairly long time interval, during which the area could have changed orientation. In order to test this possibility, overall-mean paleomagnetic directions were computed for the Paleocene–Ypresian, for the Ypresian–Lutetian and for the Lutetian–Priabonian (Table 2). The groups defined this way have practically identical declinations, documenting that the orientation of the foreland of the Southern Alps did not change during Paleocene–Eocene times.

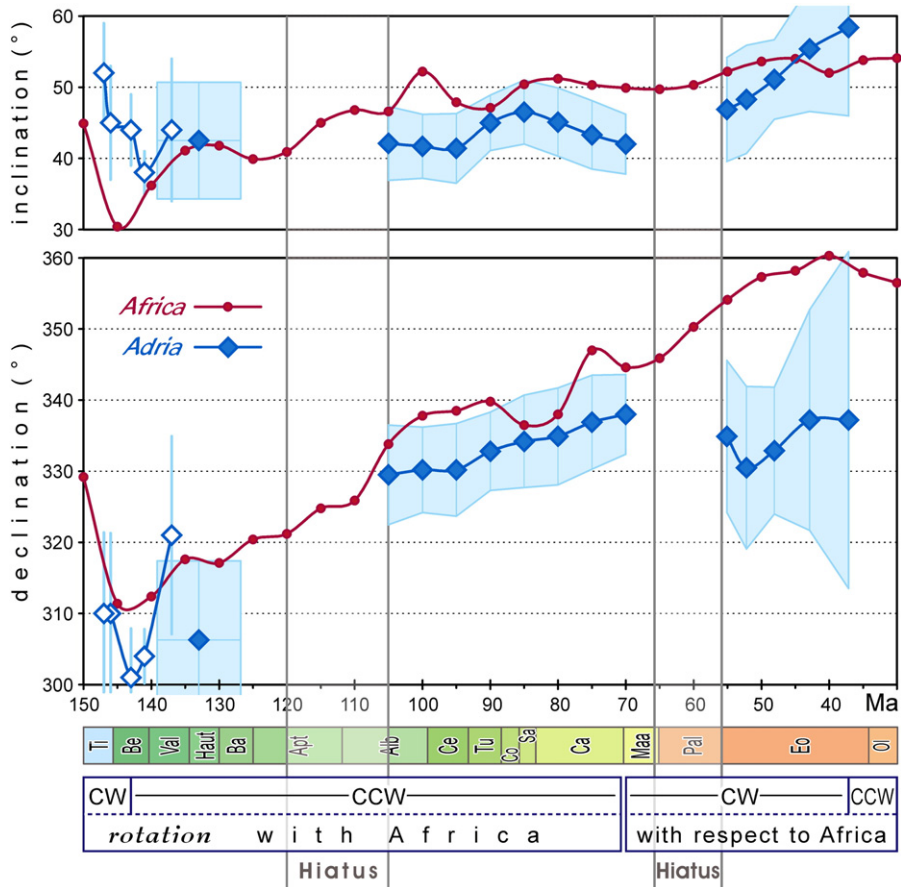


Fig. 9. Comparison of declinations/inclinations (with error bars) for stable Adria (Adige embayment and autochthonous Istria combined) with those calculated from the synthetic APW for Africa (Besse and Courtillot, 2002, 2003). Legend: in the 150–135 Ma interval, the values for Adria represent single localities (hollow diamonds), the ones plotted for younger ages are overall-mean declinations/inclinations which are based on paleomagnetic locality mean directions of relevant ages from both autochthonous study areas. The data for the time range of 115 to 37.1 Ma interval are from Table 3.

Comparison with earlier obtained Eocene paleomagnetic declinations from autochthonous Istria (based on six geographically distributed localities) does not reveal significant differences either. Thus, data from stable Istria and from the Adige embayment are combined to define a set of Paleocene–Eocene paleomagnetic directions/poles for stable Adria (Table 3) which are based on paleomagnetic locality mean directions representing a variety of lithologies.

The poles/directions thus defined significantly differ from the coeval African poles and expected directions for stable Adria, due to a CCW rotation of the former with respect to the latter (Fig. 8). Thus, the present study confirms that stable Adria decoupled from Africa after the Eocene. Unfortunately, the Oligocene and Miocene sediments from the Adige embayment failed to yield positive results. Therefore, the exact time of the Tertiary CCW rotation of stable Adria with respect to Africa remained unconstrained by recently obtained direct paleomagnetic data. Thus, the possibility of a within-Oligocene CCW rotation of the area, as suggested by Soffel (1978) cannot be excluded. Nevertheless, the CCW rotations observed on Miocene rocks in the Circum-Adriatic region call for a general driving force close to the end of Miocene (Márton, 2006) which can well be a CCW rotating Adria.

In a previous publication (Márton et al., 2010), a moderate post-Cretaceous CW rotation of stable Adria with respect to Africa was suggested, since the latest Cretaceous paleomagnetic declination from the Adige embayment and Middle/Late Eocene declination for stable Istria were similar, while the “African trend” was continuing CCW rotation. The present study provides further support to such interpretation (Fig. 9), since we have now a complete Middle Paleocene–Eocene segment of the APW for stable Adria, based on direct and consistent observations from the foreland of the Southern Alps and from autochthonous Istria.

Acknowledgment

We thank P. Grandesso for planktonic foraminifera, E. Fornaciari for calcareous nannoplankton determinations, G. Braga for initial help in field work and G. Imre for technical assistance in the field and in the laboratory. Reviews by two anonymous referees are greatly appreciated. This work was supported by the Italian–Hungarian Scientific and Technological project no. I-12/2003, the Hungarian Research Fund OTKA projects nos. K049616 and K067583 and the exchange program of the Eötvös University and the University of Padova.

References

- Abdeldayem, A.L., 1999. Paleomagnetism of some Cenozoic sediments, Cairo–Fayum area, Egypt. *Physics of the Earth and Planetary Interiors* 110, 71–82.
- Audra, P., Mocochain, L., Camus, H., Gilli, É., Clkaouz, G., Bigot, J.Y., 2004. The effect of the Messinian Deep Stage on karst development around the Mediterranean Sea. Examples from Southern France. *Geodinamica Acta* 17 (6), 389–400.
- Bassi, D., Hottinger, L., Nebelsick, J.H., 2007. Larger foraminifera from the upper Oligocene of the Venetian area, north-east Italy. *Paleontology* 50, 845–868.
- Bassi, D., Bianchini, G., Mietto, P., Nebelsick, J.H., 2008. Southern Alps in Italy: Venetian PreAlps. In: Rasser M. W. et al., 17 Palaeogene and Neogene. In McCain, T. (ed.), *The Geology of Central Europe. Vol. 2, Mesozoic and Cenozoic*. Geological Society, London, 1087–1092.
- Beccaro, L., Fornaciari, E., Mietto, P., Preto, N., 2001. Analisi di facies e ricostruzione paleoambientale dei “Calcari nummulitici” (Eocene, Monti Lessini orientali). *Studi Trentini di Scienze Naturali. Acta Geologica* 76 (1999), 3–16.
- Bertotti, G., Picotti, V., Bernoulli, D., Castellarin, A., 1993. From rifting to drifting: tectonic evolution in the South-Alpine upper crust from the Triassic to the Early Cretaceous. *Sedimentary Geology* 86, 53–76.
- Besse, J., Courtillot, V., 2002. Apparent and true polar wander and geometry of the geomagnetic field over the last 200 Myr. *Journal of Geophysical Research* 107, B11 EPM 6-1–6-31.
- Besse, J., Courtillot, V., 2003. Correction to “Apparent and true polar wander and geometry of the geomagnetic field over the last 200 Myr”. *Journal of Geophysical Research* 108, B10 EPM 3-1–3-2.
- Bigi, G., Cosentino, D., Parotto, M., Sartori, R., Scandone, P., 1990. Structural model of Italy. Sheet n. 1. In: Castellarin, A., Coli, M., Dal Piaz, G.V., Sartori, R., Scandone, P., Vai, G.B. (Eds.), *Progetto Finalizzato Geodinamica*. CNR, Roma.
- Bosellini, A., 1989. Dynamics of Tethyan Carbonate Platform. In: Crevello, et al. (Ed.), *Controls on Carbonate Platform and Basin Platform*: Society of Economic Paleontologists and Mineralogists, Special Publication, 44, pp. 3–13.
- Castellarin, A., Vai, B., Cantelli, L., 2006. The Alpine evolution of the Southern Alps around the Giudicarie faults: a Late Cretaceous to Early Eocene transfer zone. *Tectonophysics* 414, 203–223.
- Cati, A., Sartorio, D., Venturini, S., 1989. Carbonate platform in the subsurface of the Northern Adriatic area. In: Carulli, G.B., et al. (Ed.), *Evolution of the Karstic Carbonate Platform: Relation with Other Periadriatic Carbonate Platforms*: Memorie della Società Geologica Italiana, 40, pp. 295–308.
- Channell, J.E.T., De Zanche, V., Sedeo, R., 1978. Reappraisal of Palaeomagnetism of the Colli Euganei and Monti Lessini Volcanics (Italy). *Journal of Geophysics* 45, 29–33.
- Dal Piaz, G., Bistacchi, A., Massironi, M., 2003. Geological outline of the Alps. *Episodes* 26, 175–180.
- De Vecchi, G.P., Gregnanin, A., Piccirillo, E.M., 1976. Tertiary volcanism in the Veneto: magmatology, petrogenesis and geodynamic implications. *Geologische Rundschau* 65, 701–710.
- Dewey, J.F., Helman, M.L., Turco, E., Hutton, D.H.W., Knott, S.D., 1989. Kinematics of the Western Mediterranean. In: Coward, M.P., Dietrich, D., Park, R.G. (Eds.), *Alpine Tectonics*: Geological Society Special Publications London, 45, pp. 265–284.
- Doglion, C., Bosellini, A., 1987. Eoalpine and mesoalpine tectonics in the Southern Alps. *Geol. Rundsch.* 76, 735–754.
- Fantoni, R., Franciosi, R., 2009. Mesozoic extension and Cenozoic compression in Po Plain and Adriatic foreland. *Rendiconti Online della Società Geologica Italiana* 9, 28–31.
- Fisher, R.A., 1953. Dispersion on a sphere. *Proceedings of the Royal Society London* 217, 295–305.
- Frost, S.H., 1981. Oligocene reef coral biofacies of the Vicentin. 483–539. In: Toomey, D.F. (Ed.), *European Fossil Reef Models*: Society of Economic Paleontologists and Mineralogists, Sp. Publ., 30. 546 pp.
- Ghielmi, M., Minervini, M., Nini, C., Rogledi, S., Rossi, M., Vignolo, A., 2009. Sedimentary and Tectonic evolution in the Eastern Po Plain and Northern Adriatic Sea area from the Messinian to Middle Pleistocene (Italy). *Rendiconti Online della Società Geologica Italiana* 9, 32–35.
- Kafafy, A.M., Tarling, D.H., ElGamili, M.M., Hamama, H.H., Ibrahim, E.H., 1995. Contributions to the Cretaceous–Tertiary Paleomagnetism in the Nile valley, Egypt. *Proceedings of the Egyptian Academy of Sciences* 45, 121–139.
- Kirschvink, J.L., 1980. The least-squares line and plane and the analysis of paleomagnetic data. *Geophysical Journal of the Royal Astronomical Society* 62, 699–718.
- Krijgsman, W., Hilgen, F.J., Raffi, I., Sierro, F.J., Wilson, D.S., 1999. Chronology, causes and progression of the Messinian salinity crisis. *Nature* 400, 652–655.
- Kurz, W., Neubauer, F., Genser, J., Dachs, E., 1998. Alpine geodynamic evolution of passive and active continental margin sequences in the Tauern Window (Eastern Alps, Austria, Italy); a review. *Geologische Rundschau* 87, 225–242.
- Lotfy, H.I., 1999. The African Plate was still far south at the end of the Eocene: a paleomagnetic study on the late Eocene marine sediments in northeast Egypt. *Bulletin of the Faculty of Science, Assiut University* 28 (1-F), 69–83.
- Lotfy, H., Van der Voo, R., 2007. Tropical northeast Africa in the middle–late Eocene: paleomagnetism of the marine–mammals sites and basalts in the Fayum province, Egypt. *Journal of African Earth Sciences* 47, 135–152.
- Lowrie, W., 1990. Identification of ferromagnetic minerals in the rock by coercivity and unblocking temperature properties. *Geophysical Research Letters* 17, 159–162.
- Mancin, N., Cobianchi, M., Di Giulio, A., Cattelani, D., 2007. Stratigraphy of the Cenozoic subsurface succession of the Venetian–Friulian basin (NE Italy): a review. *Rivista Italiana di Paleontologia e Stratigrafia* 113 (3), 401–418.
- Márton, E., 2006. Paleomagnetic evidence for Tertiary counterclockwise rotation of Adria with respect to Africa. In: Pinter, N., Grenczy, Gy., Weber, J., Stein, S., Medak, D. (Eds.), *The Adria Microplate: GSP Geodesy, Tectonics and Hazards*. NATO Science Series IV–61, pp. 71–80.
- Márton, E., Drobne, K., Čosović, V., Moro, A., 2003. Palaeomagnetic evidence for Tertiary counterclockwise rotation of Adria. *Tectonophysics* 377, 143–156.
- Márton, E., Čosović, V., Moro, A., Zvock, S., 2008. The motion of Adria during the Late Jurassic and Cretaceous: new paleomagnetic results from stable Istria. *Tectonophysics* 454, 44–53.
- Márton, E., Zampieri, D., Grandesso, P., Čosović, V., Moro, A., 2010. New Cretaceous paleomagnetic results from the foreland of the Southern Alps and the refined apparent polar wander path for stable Adria. *Tectonophysics* 480, 57–72.
- Massari, F., Medizza, F., Sedeo, R., 1977. L’evoluzione geologica dell’area euganea tra il Giurassico superiore e l’Oligocene inferiore. In: Piccoli, G. (Ed.), *Il sistema idrotermale euganeo-berico e la geologia dei Colli Euganei*: Memorie degli Istituti di Geologia e Mineralogia dell’Università di Padova, 30, pp. 174–197.
- McFadden, P.L., 1990. A new fold test for paleomagnetic studies. *Geophysical Journal International* 103, 163–169.
- McFadden, P.L., McElhinny, M.W., 1990. Classification of the reversal test in paleomagnetism. *Geophysical Journal International* 103, 725–729.
- Ogg, J.G., Ogg, G., Gradstein, F.M., 2008. *The Concise Geologic Time Scale*. Cambridge University Press, Cambridge.
- Satolli, S., Besse, J., Speranza, F., Calamita, F., 2007. The 125–150 Ma high-resolution Apparent Polar Wander Path for Adria from magnetostratigraphic sections in Umbria–Marche (Northern Apennines, Italy): timing and duration of the global Jurassic–Cretaceous hairpin turn. *Earth and Planet Science Letters* 257, 329–342.
- Soffel, H., 1972. Anticlockwise rotation of Italy between the Eocene and Miocene. Palaeomagnetic evidence of the Colli Euganei, Italy. *Earth and Planet Science Letters* 17, 201–210.
- Soffel, H., 1974. Palaeomagnetism and rock magnetism of the Colli Euganei volcanites and the rotation of Northern Italy between Eocene and Oligocene. *Bollettino Geofisica Teorica Applicata* 16, 333–355.
- Soffel, H., 1975a. The palaeomagnetism of age dated Tertiary volcanites of the Monti Lessini (Northern Italy) and its implication to the rotation of Northern Italy. *Journal of Geophysics* 41, 385–400.

- Soffel, H., 1975b. Rock magnetism of the Monti Lessini and Monte Berici volcanites and age of volcanism deduced from the Heitzler polarity time scale. *Journal of Geophysics* 41, 401–411.
- Soffel, H., 1975c. The anticlockwise rotation of Italy during Lower Oligocene, palaeomagnetic evidence from age dated volcanics of Monte Lessini, Italy. *Rapport de la Commission Internationale pour la Mer Méditerranée* 23/4a, 59–60.
- Soffel, H., 1978. Reinterpretation of palaeomagnetism of the Colli Euganei and Monti Lessini (Italy). *Journal of Geophysics* 45, 35–39.
- Tauxe, L., Besse, J., LaBrecque, J.L., 1983. Paleolatitudes from DSDP leg 73 sedimentary cores: implications for the apparent polar wander path for Africa during the late Mesozoic and Cenozoic. *Geophysical Journal of the Royal Astronomical Society* 73, 315–324.
- Zampieri, D., 1979. Studio geologico-petrografico delle vulcaniti eoceniche della media valle del T. Chiampo (M. Lessini orientali). (Geological and petrographic study of the Eocene volcanics of the mid Chiampo valley, eastern Lessini Mountains). Unpublished Thesis, 100 pp., Padova.
- Zampieri, D., 1995. Tertiary extension in the southern Trento Platform, Southern Alps, Italy. *Tectonics* 14, 645–657.